Bioorganic & Medicinal Chemistry Letters 18 (2008) 4033–4037

Contents lists available at ScienceDirect

Bioorganic & Medicinal Chemistry Letters

journal homepage: www.elsevier.com/locate/bmcl

Structure, antimicrobial activity and DNA-binding properties of the cobalt(II)–sparfloxacin complex

Eleni K. Efthimiadou [a,b], Alexandra Karaliota [b], George Psomas [c,*]

[a] Institute of Physical Chemistry, NCSR "Demokritos", GR-15310 Aghia Paraskevi Attikis, Greece
[b] Department of Inorganic Chemistry, Faculty of Chemistry, National University of Athens, Panepistimioupoli Zographou, GR-15701 Athens, Greece
[c] Department of General and Inorganic Chemistry, Faculty of Chemistry, Aristotle University of Thessaloniki, PO Box 135, GR-54124 Thessaloniki, Greece

ARTICLE INFO

Article history:
Received 10 April 2008
Revised 30 May 2008
Accepted 31 May 2008
Available online 5 June 2008

Keywords:
Sparfloxacin
Quinolones
Cobalt(II) complex
Interaction with calf-thymus DNA

ABSTRACT

The neutral mononuclear cobalt(II) complex with sparfloxacin has been prepared and characterized with physicochemical, spectroscopic and electrochemical techniques and molecular mechanics calculations. The interaction of the complex with calf-thymus DNA has been investigated with UV spectroscopy, cyclic voltammetry and competitive studies with ethidium bromide. The antimicrobial activity of the complex has been tested against three microorganisms.

Sparfloxacin (=Hsf) (Fig. 1) is the first marketed aminodifluoroquinolone. The fluorine atom at position C-8 is thought to increase sparfloxacin's absorption and plasma half-life and its activity against Gram-positive species such as *Streptococcus pneumoniae* and Staphylococci.[1] Being a third-generation quinolone antimicrobial drug, sparfloxacin is mainly used for the treatment of acute exacerbations of chronic bronchitis and community-acquired pneumonia.[2] It has good bioavailability and its long half-life permits once-daily dosing, which may contribute to improved adherence to therapy and cost-effectiveness.[3] DNA gyrase (topoisomerase II) and topoisomerase IV are targets of sparfloxacin against *S. pneumoniae* and *Staphylococcus aureus*.[4]

The number of the sparfloxacinato metal complexes reported in the literature is, to our knowledge, quite limited. More specifically, the spectroscopic properties, the structure, the interaction with calf-thymus (CT) DNA and the biological activity of $MoO_2(sf)_2$,[5] $Cu(sf)_2$[6] and Cu(sf)(*N*-*N*)Cl (*N*-*N* = 2,2′-bipyridine, 1,10-phenanthroline(=phen) or 2,2′-bipyridylamine)[7] have been reported, as well as the crystal structures and the antiproliferative properties[8] of $Cu_2(sf)_4$ and $[Cu(Hsf)(phen)(H_2O)]^{2+}$ and the electrometric studies and magnetic measurements of a parrot-green inner complex copper(II)–sparfloxacin.[9]

An ethanolic solution (15 mL) of sparfloxacin (0.4 mmol, 157 mg), deprotonated with KOH (0.4 mmol, 22 mg), was added to an ethanolic solution (10 mL) of $CoCl_2{\cdot}6H_2O$ (0.2 mmol, 48 mg). The solution was filtered and left for slow evaporation. After a few days a yellow microcrystalline product was collected with filtration. Yield: 120 mg, 70%. The complex is soluble in methanol, DMSO and DMF and is non-electrolyte.

The absorption at 1716 cm^{-1} in the IR spectrum of Hsf attributed to the $\nu(C{=}O)_{carb}$ has been replaced with two very strong characteristic bands at 1600 and 1395 cm^{-1}, assigned as $\nu(O{-}C{-}O)$ asymmetric and symmetric stretching vibrations, respectively, whereas $\nu(C{=}O)_p$ is shifted from 1641 cm^{-1} to 1627 cm^{-1} upon bonding. The difference Δ $[=\nu(CO_2)_{asym} - \nu(CO_2)_{sym}]$ has a value of 205 cm^{-1} indicating the monodentate coordination mode of the carboxylato group.[6,10] The changes in the IR spectrum suggest

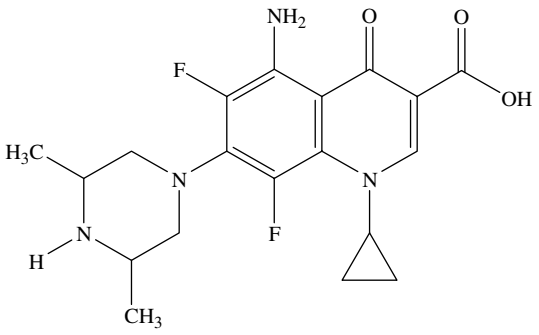

Figure 1. Sparfloxacin (Hsf = 5-amino-1-cyclohexyl-7-(*cis*-3,5-dimethylpiperazino)-6,8-difluoro-1,4-dihydro-4-oxo-3-quinolinecarboxylic acid).

* Corresponding author. Tel.: +30 2310 997790; fax: +30 2310 997738.
E-mail address: gepsomas@chem.auth.gr (G. Psomas).

0960-894X/$ - see front matter © 2008 Elsevier Ltd. All rights reserved.
doi:10.1016/j.bmcl.2008.05.115

that sparfloxacin is bound to cobalt via the pyridone oxygen and one carboxylato oxygen.[1] Finally, the band at 3405 cm^{-1} can be attributed to ν(O–H) vibration of the two coordinated water molecules.[6,10]

The UV spectrum of (**1**) is practically identical with that of sparfloxacin but slightly shifted, indicative of coordination through the pyridone and one carboxylate oxygen atom.[6] In the visible spectrum of (**1**), one band at 565 nm ($\varepsilon = 50\ M^{-1}\ cm^{-1}$) attributed to d–d transition has been found, as expected for distorted octahedral high-spin Co^{2+} complexes[11] and for a series of distorted octahedral high-spin Co^{2+} quinolone complexes.[12–16] An additional absorption band is observed as a shoulder at 430 nm ($\varepsilon = 160\ M^{-1}\ cm^{-1}$) which can be assigned to the ligand-to-metal charge-transfer transition for the quinolone ligand.[14–16]

Despite the diverse crystallization techniques employed, (**1**) was collected as microcrystalline product and its lowest energy model structure has been determined with molecular modeling calculations. Ten diastereoisomers of $Co(sf)_2(H_2O)_2$ have been constructed as starting models (Scheme S1). After the Langevin dynamics simulated annealing calculations, we obtained the total energy results of 20 different conformations for each starting model (Table S1). The average energy of each set of enantiomers is almost equal, as it is expected from such molecular mechanics calculations.[17] However, the final structures of the *transOc* isomers (Scheme 1) exhibit lower average energies by more than 1.2 kcal mol^{-1} than the other four isomers (*cis3*, *trans3*, *transOp* and *transOw*).

Applying the distance restraints (Table S2) to Co–O bonds[11–13] for the *transOc* model with the lowest energy and making corrections of the geometry by minimizing the energy of the complex once again, the structure of the predicted most stable isomer has been obtained (Fig. 2). However, we cannot exclude the formation of any of the other isomers.

The complete scan in the range +1.5 to −1.5 V of 0.4 mM methanolic solution of (**1**) shows one cathodic wave at −920 mV, two anodic waves at −745 mV and +180 mV and a second cathodic wave at −530 mV in the reverse scan. The resultant one-electron quasi-reversible waves with $E_{1/2} = -832$ mV and $\Delta E_p = 175$ mV ($E_{pc} = -920$ mV and $E_{pa} = -745$ mV) and with $E_{1/2} = -175$ mV, $\Delta E_p = 710$ mV ($E_{pc} = -530$ mV and $E_{pa} = +180$ mV) can be assigned to the couples Co(II)/Co(I) and Co(II)/Co(III), respectively.[18]

In 1:2 methanol/buffer solution (Fig. 3), one cathodic wave at −658 mV ($[Co^{II}] \rightarrow [Co^{I}]$), two anodic ones at −530 mV ($[Co^{I}] \rightarrow [Co^{II}]$) and +440 mV ($[Co^{II}] \rightarrow [Co^{III}]$) and a second cathodic wave ($[Co^{III}] \rightarrow [Co^{II}]$) at +170 mV in the reverse scan exist. The current intensities of the quasi-reversible waves attributed to the couple Co(II)/Co(I) are much higher than those of the couple Co(II)/Co(III).

DNA can provide three distinctive binding sites for quinolone metal complexes; namely, groove binding, binding to phosphate group and intercalation.[19] This behavior is of great importance with regard to the relevant biological role of quinolone antibiotics in the body.[20]

The absorption spectra of the interaction of CT DNA with (**1**), recorded for a constant CT DNA concentration (2×10^{-4} M) in different [(**1**)]/[DNA] mixing ratios (r), are shown in Figure 4A. The changes observed, that is, the increase of the intensity at $\lambda_{max} = 258$ nm up to 20% and the shift of the λ_{max} up to 265 nm, indicate that the interaction of (**1**) with CT DNA takes place by a direct formation of a new complex with CT DNA.[20] The absorption intensity at 258 nm is increased due to the fact that the purine bases and pyrimidine bases of DNA are exposed because of the binding of the complex to DNA. This kind of binding may have caused the slight change of the conformation of DNA[21] suggesting the existence of interaction.[22]

Figure 4B illustrates the spectral changes occurred in 10^{-5} M methanolic solution of (**1**) upon addition of increasing amounts of CT DNA. Even though no appreciable change in the position of the intraligand band of (**1**) is observed by addition of CT DNA, the intensity of the band centred at 302 nm is increased in the presence of DNA up to $r = 6$ and a blue shift of 10 nm (up to 292 nm) is observed for higher amounts of DNA. The hyperchromic effect observed might be ascribed to external contact (electrostatic binding)[23] or that the complex could uncoil the helix structure of DNA and made more bases embedding in DNA exposed.[24] Furthermore, one distinct isosbestic point at 300 nm exists in the spectrum as well as a new band at 267 nm appears with equal intensity to that of 302 nm.

The intrinsic binding constant K_b of (**1**) with CT DNA represents the binding constant per DNA base pair, can be obtained by monitoring the changes in absorbance at 302 nm with increasing concentrations of CT DNA from plots $\frac{[DNA]}{(\varepsilon_a - \varepsilon_f)}$ versus [DNA] (Inset of Fig. 4B) and is given by the ratio of slope to the y intercept, according to the following equation[22]:

$$\frac{[DNA]}{(\varepsilon_a - \varepsilon_f)} = \frac{[DNA]}{(\varepsilon_b - \varepsilon_f)} + \frac{1}{K_b(\varepsilon_b - \varepsilon_f)}$$

where $\varepsilon_a = A_{obsd}/[(\mathbf{1})]$, ε_f = extinction coefficient for the free complex and ε_b = extinction coefficient for (**1**) in the fully bound form. The high value of K_b obtained for (**1**) (=$2.59 \pm 0.10 \times 10^6\ M^{-1}$) suggests a strong binding of (**1**) to CT DNA. Indeed, it is much higher than K_b calculated for Hsf (=$1.71 \pm 0.02 \times 10^5\ M^{-1}$), indicating that the coordination of sparfloxacinato ligand to Co(II) ion enhances significantly the ability to bind to CT DNA. It is noteworthy that K_b of (**1**) is higher than the EB binding affinity for DNA ($K_b = 1.23 \pm 0.07 \times 10^5\ M^{-1}$) suggesting that electrostatic and intercalative interaction may affect EB displacement.[25]

The electrochemical investigations of metal–DNA interactions can provide a useful complement to spectroscopic methods, for example, for non-absorbing species, and yield information about

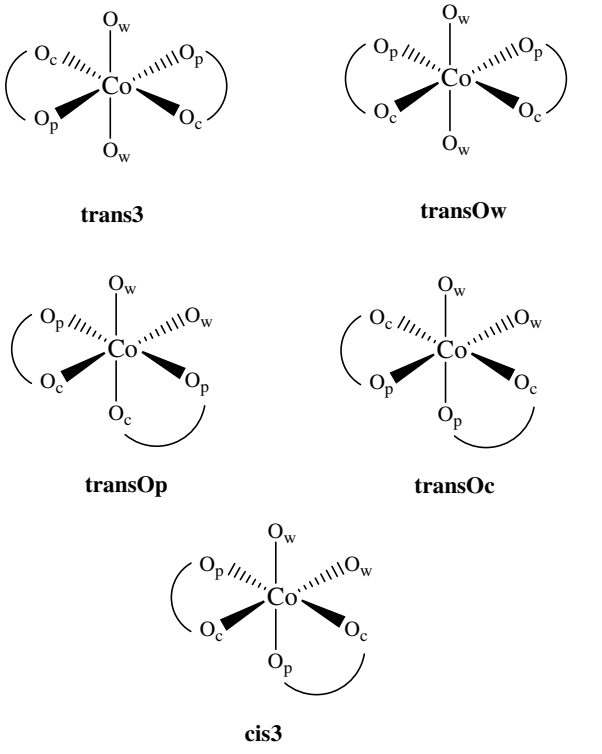

Scheme 1. The isomers of $Co(sf)_2(H_2O)_2$ employed in the simulated annealing calculations. Oc and Op are the carboxylate and the pyridone oxygen atoms, respectively, of sparfloxacin.

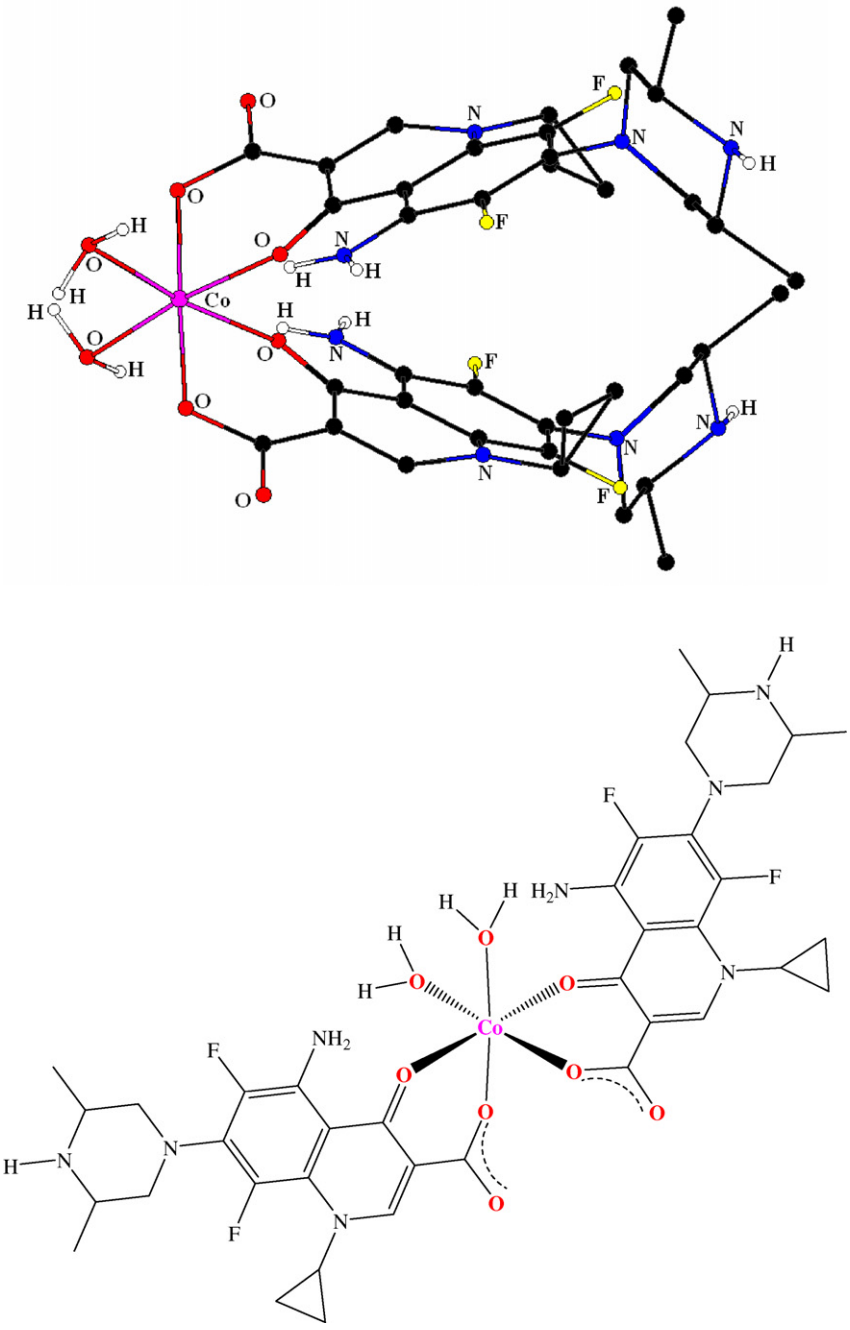

Figure 2. Lowest energy model structure for $Co(sf)_2(H_2O)_2$.

interactions with both the reduced and oxidized form of the metal.[26] No new redox peaks appeared in the cyclic voltammograms of (**1**) after the addition of CT DNA to the complex in diverse *r* values, but the current intensity of all peaks decreased significantly, suggesting the existence of an interaction between (**1**) and CT DNA (Fig. 3). The decrease in current intensity can be explained in terms of an equilibrium mixture of free and DNA-bound complex to the electrode surface.[27] For increasing amounts of CT DNA, E_{pc} shows a positive shift ($\Delta E_{pc} = +16$ mV) (indicative of intercalation)[28] while E_{pa} shifts to more negative values ($\Delta E_{pa} = -15$ mV) (indicative of electrostatic binding).[28] These shifts of the two potentials show that (**1**) can bind to DNA by both intercalation and electrostatic interaction.[29]

In order to testify that (**1**) can bind to DNA by intercalation, a competitive ethidium bromide (EB = 3,8-diamino-5-ethyl-6-phenylphenanthridinium bromide, a typical indicator of intercalation) binding study has been undertaken with fluorescence titration.[25] EB does not show any appreciable emission in buffer solution due to fluorescence quenching of the free EB by the solvent molecules.[30] On addition of CT DNA, its fluorescence intensity is highly enhanced due to its strong intercalation between the adjacent DNA base pairs.[31] Addition of a second molecule, which binds to DNA more strongly than EB, can decrease the DNA-induced EB emission.[32] The emission spectra of EB bound to CT DNA (Fig. 5A) in the absence and presence of (**1**) have been recorded for $[EB] = 2 \times 10^{-5}$ M, $[DNA] = 2.6 \times 10^{-5}$ M and increasing amounts of (**1**). The emission band at 592 nm of the DNA–EB system decreased in intensity upon addition of (**1**) at diverse *r* values up to 30% of the initial EB–DNA fluorescence intensity (Inset of Fig. 5A) indicating the competition with EB in binding

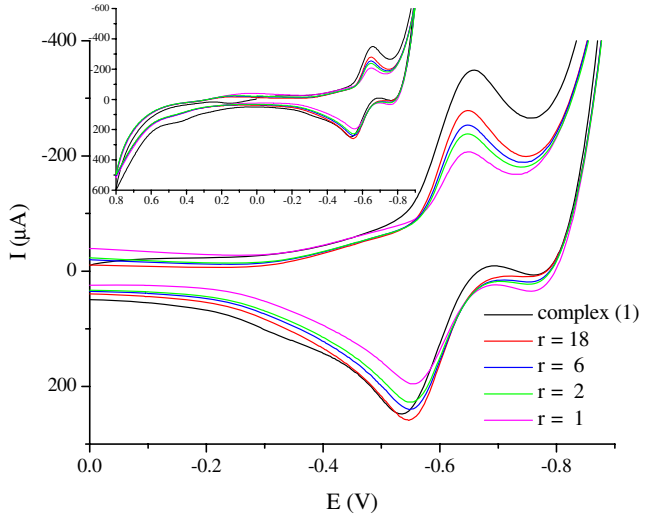

Figure 3. Cyclic voltammograms in the range 0 to −1 V of 0.4 mM of (**1**) in 1:2 methanol/buffer (containing 150 mM NaCl and 15 mM trisodium citrate at pH = 7.0) solution in the absence or presence of CT DNA in increasing amounts (r = 18 − 1) (r = [(**1**)]/[DNA]). Scan rate = 100 mV s^{-1}. Supporting electrolyte = buffer solution. (Inset) Cyclic voltammograms in the range +1 to −1 V.

to DNA. The quenching of DNA–EB fluorescence for the complex suggests that (**1**) displaces EB from the DNA–EB complex and it can interact with CT DNA by the intercalative mode.[33]

The quenching efficiency for the complex is evaluated by the Stern–Volmer constant, K_{SV}, which varies with the experimental conditions:

$$\frac{I_o}{I} = 1 + K_{SV} r$$

where I_o and I are the emission intensities in the absence and the presence of the complex, respectively.[33] The Stern–Volmer plot of DNA–EB (Fig. 5B) illustrates that the quenching of EB bound to DNA by (**1**) is in good agreement with the linear Stern–Volmer equation (R = 0.99), which proves that the partial replacement of EB bound to DNA by complex (**1**) results in a decrease in the fluorescence intensity.[27] The relatively high value of K_{SV} (=3.46) of (**1**) shows that the complex is bound very tightly to CT DNA.

The efficiencies of the ligand and the complex have been tested against two Gram(−), *Escherichia coli* and *Pseudomonas aeruginosa*, and one Gram(+), *S. aureus*, microorganisms.[34] Both the ligand and the complex have inhibitory action against all microorganisms tested and the coordination of Hsf (MIC = 0.25 − 8 μg mL^{-1}) with Co(II) results to a diverse biological activity (MIC = 1 − 4 μg mL^{-1}).

$Co(sf)_2(H_2O)$ exhibits better activity (MIC = 4 μg mL^{-1}) than Hsf (MIC = 8 μg mL^{-1}) against *E. coli* but it is less active against *P. aeruginosa* (MIC = 1 μg mL^{-1}) and *S. aureus* (MIC = 2 μg mL^{-1}) than Hsf (MIC = 0.25 and 0.5 μg mL^{-1}, respectively). $CoCl_2 \cdot 6H_2O$ does not exhibit antimicrobial activity at the concentration range used to assay the activity of the complex in this work. The chelate effect of the ligand is probably the main reason for the diverse antibacterial activity shown by the complex while the nature of the metal ion coordinated to sparfloxacinato ligand may have a significant role to this diversity,[7] for example, $Cu(sf)_2$ shows better inhibition (MIC = 0.25 − 2 μg mL^{-1}).[6]

In conclusion, the cobalt(II)–sparfloxacinato complex has been spectroscopically and electrochemically characterized and its lowest energy model structure has been determined. UV spectroscopy and cyclic voltammetry as well as competitive studies with EB with fluorescence spectroscopy have shown that $Co(sf)_2(H_2O)_2$ can bind to CT DNA by both intercalation and electrostatic interaction. Additionally (**1**) exhibits diverse antimicrobial activity against the microorganisms tested.

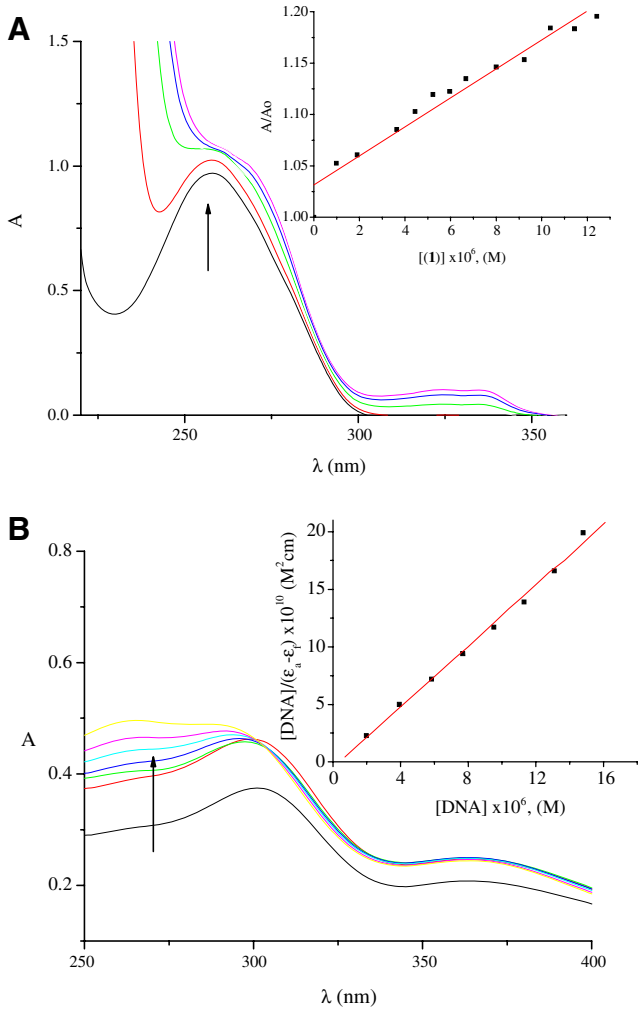

Figure 4. (A) UV spectra of CT DNA in buffer solution (150 mM NaCl and 15 mM trisodium citrate at pH = 7.0) in the presence of (**1**) at diverse r values (r = [(**1**)]/[DNA]). [DNA] = 2 × 10^{-4} M, r = 0 − 0.05. The arrow shows the intensity changes upon increasing concentration of (**1**). (Inset) Plot of A/A_o versus [(**1**)]. (B) UV spectra of (**1**) in methanolic solution in the presence of CT DNA at increasing amounts. [(**1**)] = 10 μM, [DNA] = 0–20 μM. The arrow shows the intensity changes upon increasing concentration of CT DNA. (Inset) Plot of $\frac{[DNA]}{(\varepsilon_a - \varepsilon_f)}$ versus [DNA].

Supplementary data

Experimental and materials data. Elemental analysis and spectral data for (**1**). Scheme S1 for the diastereoisomers of $Co(sf)_2(H_2O)_2$ employed in the simulated annealing calculations. Table S1 for the Co–O distance restraints applied during the energy minimization phase in order to adjust the geometry. Table S2 for the energy statistics from the simulated annealing results of $Co(sf)_2(H_2O)_2$ diastereoisomers. Supplementary data associated with this article can be found, in the online version, at doi:10.1016/j.bmcl.2008.05.115.

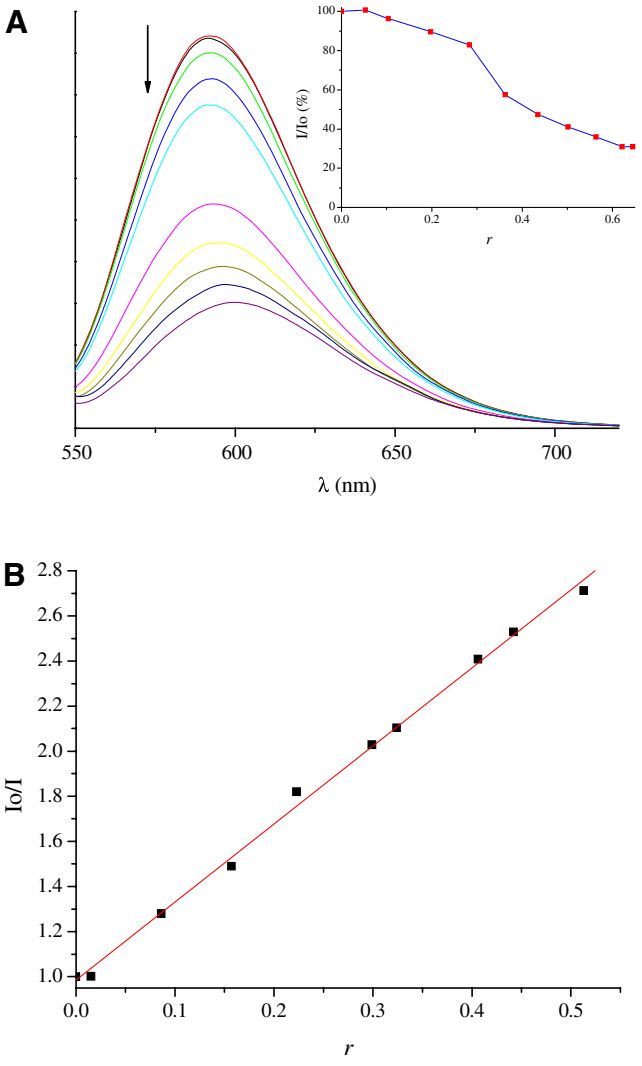

Figure 5. (A) Fluorescence spectra of EB bound to CT DNA in the absence and presence of (**1**). [EB] = 20 μM, [DNA] = 26 μM, $r = 0 - 0.6$, $\lambda_{ex} = 540$ nm. The arrow shows the intensity changes upon increasing concentration of (**1**). (Inset) Plot of EB relative fluorescence intensity (%) versus r (=[(**1**)]/[DNA]) in buffer solution (150 mM NaCl and 15 mM trisodium citrate at pH = 7.0). (B) Stern–Volmer quenching plot of EB bound to CT DNA by (**1**). $\lambda_{em} = 592$ nm.

References and notes

1. Turel, I. *Coord. Chem. Rev.* **2002**, *232*, 27.
2. King, D. E.; Malone, R.; Lilley, S. H. *Am. Fam. Physician* **2000**, *61*, 2741.
3. Schentag, J. J. *Clin. Ther.* **2000**, *22*, 372.
4. Pan, X. S.; Fisher, L. M. *Antimicrob. Agents Chemother.* **1997**, *41*, 471.
5. Efthimiadou, E. K.; Karaliota, A.; Psomas, G. *Polyhedron* **2008**, *27*, 349.
6. Efthimiadou, E. K.; Sanakis, Y.; Raptopoulou, C. P.; Karaliota, A.; Katsaros, N.; Psomas, G. *Bioorg. Med. Chem. Lett.* **2006**, *16*, 3864.
7. Efthimiadou, E. K.; Katsarou, M. E.; Karaliota, A.; Psomas, G. *J. Inorg. Biochem.* **2008**, *102*, 910.
8. Shingnapurkar, D.; Butcher, R.; Afrasiabi, Z.; Sinn, E.; Ahmed, F.; Sarkar, F.; Padhye, S. *Inorg. Chem. Commun.* **2007**, *10*, 459.
9. Gupta, S.; Ansari, M. N. *J. Inst. Chem. (India)* **2001**, *73*, 154; Gupta, S.; Ansari, M. N. *Chem. Abstr.* **2002**, *136*, 349739.
10. Nakamoto, K. *Infrared and Raman Spectra of Inorganic and Coordination Compounds*, fourth ed.; Wiley: New York, 1986.
11. Garoufis, A.; Kasselouri, S.; Raptopoulou, C. P. *Inorg. Chem. Commun.* **2000**, *3*, 251.
12. Jimenez-Garrido, N.; Perello, L.; Ortiz, R.; Alzuet, G.; Gonzalez-Alvarez, M.; Canton, E.; Liu-Gonzalez, M.; Garcia-Granda, S.; Perez-Priede, M. *J. Inorg. Biochem.* **2005**, *99*, 677.
13. Lopez-Gresa, M. P.; Ortiz, R.; Perello, L.; Latorre, J.; Liu-Gonzalez, M.; Garcia-Granda, S.; Perez-Priede, M.; Canton, E. *J. Inorg. Biochem.* **2002**, *92*, 65.
14. Efthimiadou, E. K.; Psomas, G.; Sanakis, Y.; Katsaros, N.; Karaliota, A. *J. Inorg. Biochem.* **2007**, *101*, 525.
15. Tarushi, A.; Christofis, P.; Psomas, G. *Polyhedron* **2007**, *26*, 3963.
16. Efthimiadou, E. K.; Karaliota, A.; Psomas, G. *Polyhedron* **2008**, *27*, 1729.
17. Christofis, P.; Katsarou, M.; Papakyriakou, A.; Sanakis, Y.; Katsaros, N.; Psomas, G. *J. Inorg. Biochem.* **2005**, *99*, 2197.
18. Papadopoulos, C. D.; Hatzidimitriou, A. G.; Voutsas, G. P.; Lalia-Kantouri, M. *Polyhedron* **2007**, *26*, 1077.
19. Zeglis, B. M.; Pierre, V. C.; Barton, J. K. *Chem. Commun.* **2007**, 4565.
20. Son, G. S.; Yeo, J.-A.; Kim, M.-S.; Kim, S. K.; Holmen, A.; Akerman, B.; Norden, B. *J. Am. Chem. Soc.* **1998**, *120*, 6451.
21. Song, Y.-M.; Wu, Q.; Yang, P.-J.; Luan, N.-N.; Wang, L.-F.; Liu, Y.-M. *J. Inorg. Biochem.* **2006**, *100*, 1685.
22. Pyle, A. M.; Rehmann, J. P.; Meshoyrer, R.; Kumar, C. V.; Turro, N. J.; Barton, J. K. *J. Am. Chem. Soc.* **1989**, *111*, 3053.
23. Pasternack, R. F.; Gibbs, E. J.; Villafranca, J. J. *Biochemistry* **1983**, *22*, 2406.
24. Pratviel, G.; Bernadou, J.; Meunier, B. *Adv. Inorg. Chem.* **1998**, *45*, 251.
25. Dimitrakopoulou, A.; Dendrinou-Samara, C.; Pantazaki, A. A.; Alexiou, M.; Nordlander, E.; Kessissoglou, D. P. *J. Inorg. Biochem.* **2008**, *102*, 618.
26. Carter, M. T.; Bard, A. J. *J. Am. Chem. Soc.* **1987**, *109*, 7528.
27. Tabassum, S.; Parveen, S.; Arjmand, F. *Acta Biomater.* **2005**, *1*, 677.
28. Carter, M. T.; Rodriguez, M.; Bard, A. J. *J. Am. Chem. Soc.* **1989**, *111*, 8901.
29. Jiao, K.; Wang, Q. X.; Sun, W.; Jian, F. F. *J. Inorg. Biochem.* **2005**, *99*, 1369.
30. Dhar, S.; Nethaji, M.; Chakravarty, A. R. *J. Inorg. Biochem.* **2005**, *99*, 805.
31. Olmsted, J.; Kearns, D. R. *Biochemistry* **1977**, *16*, 3647.
32. Baguley, B. C.; Lebret, M. *Biochemistry* **1984**, *23*, 937.
33. Novakova, O.; Chen, H.; Vrana, O.; Rodger, A.; Sadler, P. J.; Brabec, V. *Biochemistry* **2003**, *42*, 11544.
34. The lowest concentration that inhibited bacterial growth was determined as the MIC value. More details are given in Supplementary material.